

# Soft/hard exchange-coupled layered structures with modulated exchange coupling

Shi-Shen Yan<sup>a)</sup>

Department of Mechanical Engineering, FAMU-FSU COE, 2525 Pottsdamer Road, RM 229, Tallahassee, Florida 32310 and School of Physics and Microelectronics, Shandong University, Jinan, Shandong, 250100, Peoples Republic of China

M. Elkawni, D. S. Li, and H. Garmestani

Department of Mechanical Engineering, FAMU-FSU COE, 2525 Pottsdamer Road, RM 229, Tallahassee, Florida 32310

J. P. Liu

Department of Physics, University of Texas at Arlington, Arlington, Texas 76019

J. L. Weston and G. Zangari

MINT, The University of Alabama, Box 870209, Tuscaloosa, Alabama 35487-0209

(Received 8 April 2003; accepted 28 June 2003)

Magnetically soft/hard exchange-coupled  $\text{Ni}_{80}\text{Fe}_{20}/\text{Si}_3\text{N}_4/\text{Sm}_{40}\text{Fe}_{60}$  and  $\text{Ni}_{80}\text{Fe}_{20}$ /mixture/ $\text{Sm}_{40}\text{Fe}_{60}$  layered structures with induced in-plane uniaxial anisotropy were deposited by sputtering on Si (100) substrates. The interfacial exchange coupling strength between the soft and hard layers was tailored by inserting a thin nonmagnetic insulating  $\text{Si}_3\text{N}_4$  layer or by varying interfacial mixture of NiFe and SmFe. It was found that the reduction in the exchange coupling greatly reduces the nucleation field  $H_N$  of the soft layer and increases the irreversible switching field  $H_{\text{irr}}$  of the hard layer. The simple formula used before to describe the nucleation field of the soft layer does not work in the case of the reduced interfacial exchange coupling. © 2003 American Institute of Physics. [DOI: 10.1063/1.1604931]

## I. INTRODUCTION

Many efforts have been devoted to the search for high performance permanent magnets in the past decades and much progress has been made in improving permanent magnetic properties. A figure of merit of permanent magnetic materials is the maximum magnetic energy product  $(BH)_{\text{max}}$ . The highest value of the energy product  $(BH)_{\text{max}} = 56 \text{ MG Oe}$  has so far been achieved for NdFeB-based magnets, which is close to the theoretical upper limit  $\mu_0 M_S^2/4 = 65 \text{ MG Oe}$  of this material system. Therefore, it seems that there is little room left for improving the magnetic energy product within the frame of conventional single-phase hard magnets.

In order to overcome the limitation of the saturation magnetization of single magnetic hard phases, Kneller *et al.*<sup>1</sup> proposed a concept of oriented nanostructured two-phase magnets (also called exchange-spring magnets). It is predicted that a magnetic energy product as high as 125 GM Oe is achievable for suitable nanostructured SmFeN/FeCo composites.<sup>2</sup> The attractive value of this large energy product is more than doubling the highest energy product (56 MG Oe) achieved in NdFeB. According to this concept, the surplus high coercivity of the hard phase and the high magnetization of the soft phase can be combined in an exchange-spring magnet due to strong exchange coupling between the two phases. In this way the composite magnet can show a hysteresis loop like a single hard phase does, but with a much larger energy product.

Stimulated by the predicted high energy product, many recent investigations have been focused on layered exchange spring systems<sup>3-6</sup> which can be traced back to about 40 years ago.<sup>7</sup> To date, the magnetization reversal process of the soft layer in exchange spring systems seems to be well understood, but the magnetic reversal mechanism of the hard layer is still poorly known.<sup>3-5</sup> On the other hand, little attention has been paid to how the exchange coupling strength between the hard and soft phases influences the nucleation field of the soft layer and the irreversible switching field of the hard layer,<sup>2-7</sup> although a strong interfacial exchange coupling is a prerequisite to achieve high magnetic energy product of exchange spring systems. Moreover, the theoretically predicted high energy product in nanostructured systems<sup>2</sup> has not yet been achieved in experiments, and this is probably related to imperfect interface coupling.

In this article, we report the influence of the interfacial exchange coupling strength on the switching fields of the soft and the hard layers in a model exchange-spring system. We investigated  $\text{Ni}_{80}\text{Fe}_{20}/\text{Si}_3\text{N}_4/\text{Sm}_{40}\text{Fe}_{60}$  sandwich structures, where NiFe is the soft layer, SmFe is the hard layer, and the nonmagnetic insulating  $\text{Si}_3\text{N}_4$  layer is inserted to modulate the coupling strength between the two magnetic layers. The nonmagnetic insulating  $\text{Si}_3\text{N}_4$  layer, rather than nonmagnetic metal layers such as Cu, Ag, and Au, was chosen because a monotonous reduction of the coupling strength with the increased layer thickness of the nonmagnetic insulator is expected. The interfacial coupling strength was also modified by intentional interfacial mixture induced during sputtering and postannealing.

<sup>a)</sup> Author to whom correspondence should be addressed; electronic mail: shishenyan@yahoo.com

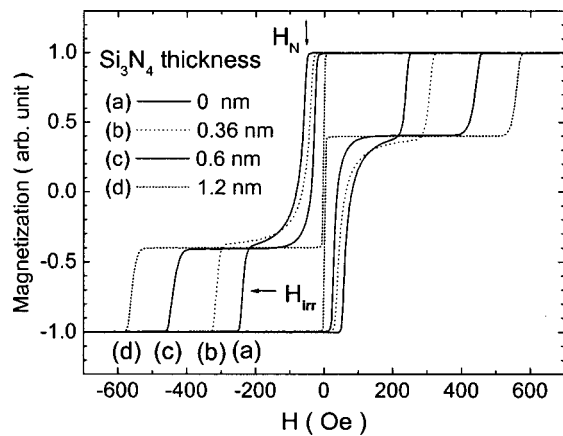


FIG. 1. Some typical easy-axis magnetization hysteresis loops of  $\text{Ni}_{80}\text{Fe}_{20}$  (63 nm)/ $\text{Si}_3\text{N}_4$ /Sm $_{40}\text{Fe}_{60}$  (78 nm) sandwiches with various  $\text{Si}_3\text{N}_4$  thicknesses. The thicknesses of the nonmagnetic insulating  $\text{Si}_3\text{N}_4$  layer are (a) 0, (b) 0.36, (c) 0.6, and (d) 1.2 nm, respectively. The nucleation field  $H_N$  of the magnetically soft layer and the irreversible switching field  $H_{\text{irr}}$  of the magnetically hard layer are marked for Fig. 1(a).

## II. EXPERIMENTS

$\text{Ni}_{80}\text{Fe}_{20}$ / $\text{Si}_3\text{N}_4$ /Sm $_{40}\text{Fe}_{60}$  sandwiches of various thicknesses were prepared on (100)-Si substrates by sputtering. The magnetic  $\text{Ni}_{80}\text{Fe}_{20}$  and Sm $_{40}\text{Fe}_{60}$  layers were deposited by dc magnetron sputtering at the growth rates of 0.15 and 0.16 nm/s, respectively, and the insulating  $\text{Si}_3\text{N}_4$  layer was deposited by rf sputtering at a very low growth rate of 0.06 nm/s. The pressure of the Ar gas was stabilized at 3 mTorr during the sputtering process. To induce an in-plane uniaxial anisotropy, two permanent magnets were used to supply an external magnetic field of 80 Oe in the film plane during film deposition. Finally, an additional 5 nm  $\text{Si}_3\text{N}_4$  layer was deposited on the top of the sandwiches as the protective layer. The high-angle x-ray diffraction patterns indicate that the NiFe layer exhibits fcc (111) crystalline texture and the SmFe layer is amorphous. The magnetization hysteresis loops were measured along the easy axis direction by alternating gradient magnetometry (AGM) and/or vibrating sample magnetometry. In order to reduce the error of the coercivity value to a minimum, a very small magnetic field gradient of 0.4 Oe/mm was used in the AGM measurements. The samples were sealed in a vacuum tube of the quartz glass for the magnetic annealing to avoid oxidization.

## III. EXPERIMENTAL RESULTS AND DISCUSSION

Figure 1 shows typical easy-axis magnetization hysteresis loops of  $\text{Ni}_{80}\text{Fe}_{20}$  (63 nm)/ $\text{Si}_3\text{N}_4$ /Sm $_{40}\text{Fe}_{60}$  (78 nm) sandwiches with various  $\text{Si}_3\text{N}_4$  thicknesses. A detailed description of the whole magnetization reversal process can be given based on the hysteresis loops. For loops of Figs. 1(a)–1(c), two characteristic switching fields, i.e., the nucleation field  $H_N$  of the magnetically soft layer and the irreversible switching field  $H_{\text{irr}}$  of the magnetically hard layer, clearly show the exchange spring feature of the magnetization reversal. After reaching magnetization saturation along the easy axis and then reversing the field exceeding the nucleation field  $H_N$  of the soft layer, the magnetic moments in the soft NiFe layer begin to continuously twist across the soft NiFe

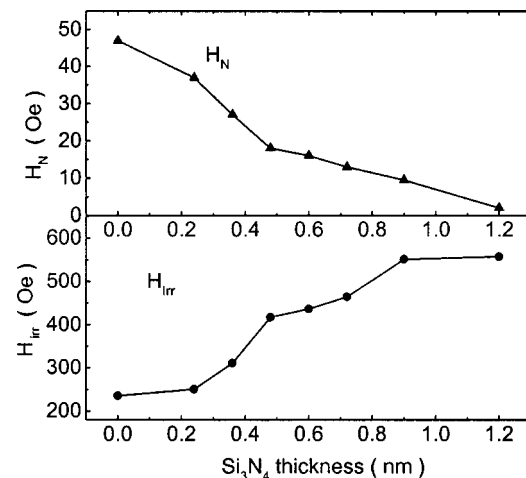


FIG. 2. The nucleation field  $H_N$  of the soft NiFe layer and the irreversible switching field  $H_{\text{irr}}$  of the hard SmFe layer versus the nonmagnetic insulating  $\text{Si}_3\text{N}_4$  layer thickness for  $\text{Ni}_{80}\text{Fe}_{20}$  (63 nm)/ $\text{Si}_3\text{N}_4$ /Sm $_{40}\text{Fe}_{60}$  (78 nm) sandwiches.

layer, similar to the case of a single in-plane magnetic domain wall. With increasing reversal field from  $H_N$  to  $H_{\text{irr}}$ , the in-plane domain wall is compressed against the interfacial region of the soft/hard layers, but the magnetic moments in the magnetically hard SmFe layer are still fixed along the previous saturation direction. This magnetization reversal process from  $H_N$  to  $H_{\text{irr}}$  is completely reversible, and it is usually called exchange spring phenomenon. To date, the exchange-spring process based on a single in-plane domain wall picture seems to have been well understood in experiments and theoretical calculations.<sup>3–6</sup> However, our recent magnetic domain observation<sup>8</sup> indicated that the exchange-spring process was caused by the simultaneously clockwise and counterclockwise twist on a local scale when the external field is precisely along the easy axis, rather than the simple case as a single in-plane domain wall. As for the irreversible magnetization reversal at  $H_{\text{irr}}$ , it is generally regarded that the strongly compressed in-plane domain wall is unpinned at the interface region and crosses the hard layer thickness.<sup>4,6</sup> However, our magnetic domain observation indicates that the above process only occurred locally and produced a reverse magnetic nucleus. Then the nucleus quickly grew laterally (in the plane of the film) by the motion of domain walls. So the irreversible magnetization reversal at  $H_{\text{irr}}$  was caused by nucleation of the reversal magnetic domains and successive domain wall motion in the plane of the film.<sup>8</sup> For the loop of Fig. 1(d), the soft NiFe layer and the hard SmFe layer show the respective coercivity of the isolated single layers. This means that the exchange coupling between the soft NiFe layer and the hard SmFe layer becomes negligibly small in Fig. 1(d) when the  $\text{Si}_3\text{N}_4$  layer thickness is more than 1.2 nm.

Figure 1 indicates that the nucleation field  $H_N$  of the magnetically soft layer quickly reduces and the irreversible switching field  $H_{\text{irr}}$  of the magnetically hard layer quickly increases with increasing the  $\text{Si}_3\text{N}_4$  layer thickness (i.e., with reducing the exchange coupling strength). This trend was highlighted in Fig. 2. When no  $\text{Si}_3\text{N}_4$  layer was inserted between  $\text{Ni}_{80}\text{Fe}_{20}$  and Sm $_{40}\text{Fe}_{60}$  layers, the soft layer and

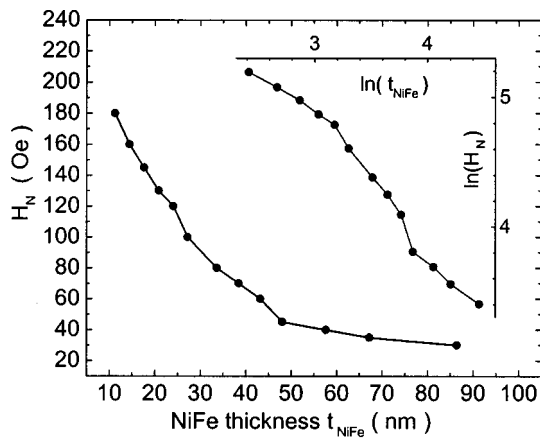


FIG. 3. The nucleation field  $H_N$  of the soft NiFe layer vs the NiFe layer thickness  $t$  for the  $\text{Ni}_{80}\text{Fe}_{20}$  (10–86 nm)/ $\text{Si}_3\text{N}_4$  (0.36 nm)/ $\text{Sm}_{40}\text{Fe}_{60}$  (81.4 nm) sandwiches. The inset shows the dependence of  $\ln(H_N)$  on  $\ln(t)$ .

hard layer have the strongest coupling through the direct exchange interaction. So the nucleation field  $H_N$  of the soft layer reaches a maximum and the irreversible switching field  $H_{\text{irr}}$  of the hard layer reaches a minimum. When a very thin nonmagnetic insulating  $\text{Si}_3\text{N}_4$  layer was added in between, the soft layer and hard layer may couple by three mechanisms, i.e., direct coupling through the magnetic bridges in  $\text{Si}_3\text{N}_4$  layer (pin hole effect), indirect coupling through quantum tunneling effect, and magnetic dipolar interaction. Since the two magnetic layers decouple when the  $\text{Si}_3\text{N}_4$  layer thickness is increased to 1.2 nm, these interactions reduce very quickly with increasing the thickness of  $\text{Si}_3\text{N}_4$  layer. The strongly reduced coupling by a thin nonmagnetic insulating layer implies that for randomly dispersed nanocomposite soft-hard two phases magnets such as the  $\text{Nd}_2\text{Fe}_{14}\text{B}/\alpha\text{-Fe}$  composite, the nonmagnetic B-riched phase should be avoided in between the soft and hard phases to achieve a high magnetic energy product.

The nucleation field  $H_N$  of the soft layer versus the NiFe layer thickness is shown in Fig. 3 for  $\text{Ni}_{80}\text{Fe}_{20}$  (10–86 nm)/ $\text{Si}_3\text{N}_4$  (0.36 nm)/ $\text{Sm}_{40}\text{Fe}_{60}$  (81.4 nm) sandwiches. In these samples, the SmFe layer thickness is fixed at 81.4 nm and a 0.36 nm  $\text{Si}_3\text{N}_4$  layer was added in between to reduce the exchange coupling. It is clear that the nucleation field  $H_N$  gradually reduces with increasing the soft layer thickness  $t$ . However, the relation between  $H_N$  and  $t$  cannot be described by an empirical formula<sup>3,5,7</sup>

$$H_N = H_{N0}/t^n, \tag{1}$$

where  $H_{N0}$  and  $n$  are two constants for a given soft/hard exchange-coupled system. This can be seen from the inset in Fig. 3, where  $\ln(H_N) - \ln(t)$  relation is not linear. Otherwise,  $\ln(H_N) - \ln(t)$  curve will show linear behavior if Eq. (1) can well describe the present experimental data. It is well known that Eq. (1) can well describe the experimental results of soft/hard exchange-coupled systems<sup>3,5,7</sup> if no nonmagnetic insulating layer was added between the soft layer and the hard layer (i.e., in the case of strong exchange coupling).

In particular, if the soft layer has no anisotropy and the interface moments are perfectly rigid, theory predicts<sup>7</sup> that Eq. (1) is in the form of

$$H_N = \pi^2 A / 2M_S t^2, \tag{2}$$

where  $A$  and  $M_S$  are, respectively, the exchange constant and the saturation magnetization of the soft layer [i.e.,  $H_{N0} = \pi^2 A / 2M_S$ , and  $n = 2$  in Eq. (1)]. According to Eq. (2), the nucleation field of the soft layer in  $\text{Ni}_{80}\text{Fe}_{20}$  (63 nm)/ $\text{Sm}_{40}\text{Fe}_{60}$  (78 nm) bilayer is expected to be 116 Oe if  $A = 0.8 \times 10^{-6}$  erg/cm (taking the value in Ref. 7 for NiFe layer),  $M = 856$  emu/cm<sup>3</sup>, and  $t = 6.3 \times 10^{-6}$  cm (experimental values) are used. However, the experimental value is  $H_N = 49$  Oe (see Fig. 1). This means that the interfacial moments are far from the rigid assumption in NiFe/SmFe bilayer. The nonrigid interfacial moments means that the interfacial exchange coupling is not strong enough as compared with the exchange coupling inside the NiFe soft layer, and/or that the anisotropy (or coercivity) of the SmFe hard layer is not strong enough.

On the other hand, if the interfacial coupling  $J$  between the soft layer and the hard layer is weak (for example, by inserting a nonmagnetic insulating  $\text{Si}_3\text{N}_4$  interlayer) as compared with the exchange coupling inside the soft layer and the hard layer, the nucleation field of the soft layer (or the switching field) in the form of  $H_N = J/M_S t$  [i.e.,  $H_{N0} = J/M_S$ , and  $n = 1$  in Eq. (1)] can be directly deduced. However, when the interfacial exchange coupling strength is in between the two extreme cases (strong exchange coupling and weak exchange coupling), no analytical expression has been given to describe the nucleation field of the soft layer. Our experimental results indicate that Eq. (1) can not be used to describe the nucleation field of the magnetically soft layer when the exchange coupling was reduced by inserting a nonmagnetic insulating layer between the soft layer and the hard layer, although it really works in many other cases.

Interfacial exchange coupling was also varied by intentionally mixing NiFe and SmFe in the interfacial region. The thickness of the intentional mixture was controlled by alternately depositing very thin NiFe and SmFe layers at the interface and then annealing the samples. Here the nominal mixed region has the structure of  $[\text{SmFe} (0-1 \text{ nm})/\text{NiFe} (0-1 \text{ nm})] \times 2$ , which is inserted between the interface of the NiFe (63 nm)/SmFe (78 nm) bilayer. In order to keep a good uniaxial in-plane anisotropy and significant interfacial mixture, we annealed samples in a high magnetic field of  $24 \times 10^4$  Oe at 200 °C for 3 h. In this case the nominal thickness of the mixture was regarded as the sum of the very thin NiFe and SmFe layer thicknesses.

Figure 4 shows the hysteresis loops of the samples with various mixture thicknesses. The nominal mixture thickness inserted in the interface are, respectively, 0, 2.5 nm [i.e.,  $[\text{SmFe} (0.64 \text{ nm})/\text{NiFe} (0.61 \text{ nm})] \times 2$ ], and 3.8 nm [i.e.,  $[\text{SmFe} (0.98 \text{ nm})/\text{NiFe} (0.92 \text{ nm})] \times 2$ ], which are very small as compared with the 63 nm NiFe layer and 78 nm SmFe layer. Before the magnetic annealing, all the loops for various nominal mixture thicknesses from 0 to 3.8 nm are almost the same as Fig. 4(a), which is a loop of the as-deposited NiFe (63 nm)/SmFe (78 nm) bilayer without intentional mixture. It looks strange that the inserted interfacial mixture layers cannot show detectable differences in the loops before the magnetic annealing. It is reasonable if we

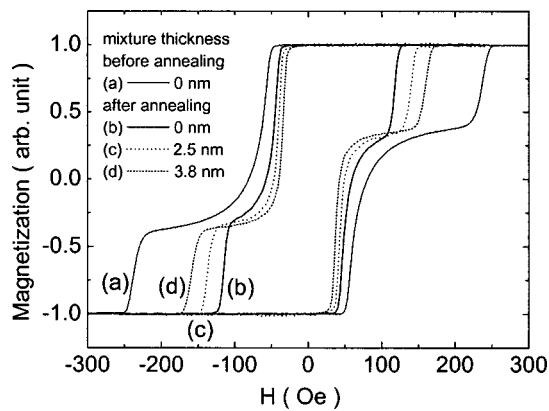


FIG. 4. The hysteresis loops of NiFe (63 nm)/mixture/SmFe (78 nm) samples with various mixture thicknesses. Figure 4(a) is the loop of the NiFe (63 nm)/SmFe (78 nm) bilayer (without intentional mixture) before magnetic annealing, and Fig. 4(b) is the loop of the same sample after magnetic annealing. Figures 4(c) and 4(d) are the hysteresis loops of the magnetic annealed samples with the intentional mixture thicknesses of 2.5 and 3.8 nm, respectively.

believe that the interfacial coupling strength at all the interfaces between the NiFe and SmFe layers is the same and strong. In this case, the inserted interfacial mixture layers can couple together and show intermediate (or average) magnetization and anisotropy, but still with the same interfacial coupling strength at the interfaces. Even if one regards the relatively thin inserted interfacial mixture layers as a very little increase in the soft NiFe layer thickness or on the contrary as a very little increase in the hard SmFe layer thickness, it cannot show obvious changes in the loops when the interfacial coupling does not change. This is because hysteresis loop measurements are not sensitive to the local magnetization and anisotropy when exchange coupling is strong between different magnetic phases, but sensitive to the local coupling strength between different magnetic phases, especially the weakest local coupling in the system.

After the magnetic annealing, the hysteresis loops for the intentional mixture thicknesses of 0, 2.5, and 3.8 nm are, respectively, shown in Figs. 4(b), 4(c), and 4(d). From Figs. 4(a) to 4(b) (the nominal mixture thickness is 0), both the nucleation field of the magnetically soft NiFe layer and the irreversible switching field of the magnetically hard SmFe layer greatly reduced after the magnetic annealing. As analyzed earlier, the interfacial mixture caused by the magnetic annealing may lead to the intermediate magnetization and anisotropy in the mixed region, but it can not lead to obvious changes in the loops if the effective interfacial coupling does not change. Hence, we believe that the magnetic annealing enhanced the interfacial mixture and weakened the effective exchange coupling between NiFe and SmFe layers. As a result  $H_N$  reduced after the magnetic annealing. If we assume the interfacial mixed region is SmFeNi alloy, it implies that the exchange coupling within the SmFeNi alloy is weaker than the initial interfacial coupling between the NiFe and SmFe layers.

As mentioned in the previous section, in our samples SmFe layers are amorphous and the in-plane uniaxial anisotropy

is induced during the film growth at room temperature. The induced anisotropy can be re-established by magnetic annealing and it usually reduces with increasing magnetic annealing temperature (below the crystallization temperature). Correspondingly, the easy-axis coercivity of the magnetically hard SmFe layers also reduces with increasing magnetic annealing temperature. Therefore, although the reduced interfacial exchange coupling had the tendency to increase  $H_{irr}$ , the  $H_{irr}$  was still greatly reduced after the magnetic annealing.

Comparing Figs. 4(b), 4(c), and 4(d), we found that  $H_N$  decreases and  $H_{irr}$  increases with increasing the mixture thickness, which is similar to the case of increasing the nonmagnetic insulating  $\text{Si}_3\text{N}_4$  layer thickness [see Figs. 1(a)–1(d)]. This means that the increased interfacial mixture influences  $H_N$  and  $H_{irr}$  mainly by reducing the effective exchange coupling between NiFe and SmFe layers although it may also change the anisotropy and magnetization of the interfacial mixture region. However, the changes in  $H_N$  and  $H_{irr}$  caused by the intentional interfacial mixture are not as significant as those caused by inserting a nonmagnetic insulating  $\text{Si}_3\text{N}_4$  layer.

#### IV. CONCLUSIONS

In summary, the influence of the interfacial exchange coupling on the magnetization reversal in the soft/hard exchange-coupled NiFe/SmFe system was studied. The interfacial exchange coupling was modulated by inserting a very thin nonmagnetic insulating  $\text{Si}_3\text{N}_4$  layer between the two magnetic layers or by varying interfacial mixture. It was found that the reduced exchange coupling always reduces  $H_N$  and increases  $H_{irr}$ . The simple formula [Eq. (1)] adopted before to describe the nucleation field of the soft layer cannot be used in the case of the reduced interfacial exchange coupling. Our studies indicate that nonmagnetic components and interfacial mixture between the soft and hard phases should be avoided in nanostructured exchange spring bulk magnets in order to maintain a strong exchange coupling to achieve high magnetic energy product.

#### ACKNOWLEDGMENTS

This work was supported by DARPA No. DAAD19-01-1-0546 and Army Grant Nos. DAAD19-01-1-0742 and MRSEC-DMR-0213985.

<sup>1</sup>E. F. Kneller and R. Hawig, IEEE Trans. Magn. **27**, 3588 (1991).

<sup>2</sup>R. Skomski and J. M. D. Coey, Phys. Rev. B **48**, 15812 (1993).

<sup>3</sup>T. Nagahama, K. Mibu, and T. Shinjo, J. Phys. D **31**, 43 (1998).

<sup>4</sup>E. E. Fullerton, J. S. Jiang, M. Grimsditch, C. H. Snowers, and S. D. Bader, Phys. Rev. B **58**, 12193 (1998).

<sup>5</sup>S.-S. Yan, J. A. Barnard, F.-T. Xu, J. L. Weston, and G. Zangari, Phys. Rev. B **64**, 184403 (2001).

<sup>6</sup>S. Mangin, G. Marchal, C. Bellouard, W. Wernsdorfer, and B. Barbara, Phys. Rev. B **58**, 2748 (1998).

<sup>7</sup>E. Goto, N. Hayashi, T. Miyashita, and K. Nakagawa, J. Appl. Phys. **36**, 2951 (1965).

<sup>8</sup>D. Chumakov, R. Schäfer, D. Elefant, D. Eckert, L. Schultz, S. S. Yan, and J. A. Barnard, Phys. Rev. B **66**, 134409 (2002).